CONSTRUCTION
E-ISSN: 2785-8731
VOLUME 3, ISSUE 2, 2023, 152 – 162
DOI: https://doi.org/10.15282/construction.v3i2.9383

RESEARCH ARTICLE

The Effect of Concrete Cover Thickness on the Torsional Resistance of Fibrous, High-strength, Under-reinforced Concrete Beams

F. R. Karim[1]*, B. H. Abu Bakar[2], C. K. Keong[2], and O. Q. Aziz[3]

[1]College of Engineering, Civil Engineering Department, University of Sulaimani, Sulaimani, Iraq
[2]School of Civil Engineering, Universiti Sains Malaysia, Pulau Pinang, Malaysia
[3]College of Engineering, Civil Engineering Department, University of Salahaddin, Erbil, Iraq

ABSTRACT - This study focuses on the role of concrete cover in enhancing the torsional resistance of peak load in under-reinforced fibrous high-strength concrete beams. In this study, the primary variable that varied from 17 mm to 53 mm was the concrete cover thickness. Four rectangular solid beams were cast and tested to determine the effect of concrete cover thickness on the behaviour of under-reinforced fibrous, high strength concrete beams subjected to pure torsional loading. The test results revealed an 80.6% improvement in the torsional resistance at peak load. In addition, at maximal loads, the twisting angle, shear strain in concrete, transverse reinforcement strain, and longitudinal reinforcement strain were reduced by 70.2%, 90%, 50.6%, and 34.5%, respectively. It is therefore possible to draw the conclusion that the concrete cover has a new function, which is an improvement in torsional resistance at ultimate load that is in addition to protecting the reinforcement from corrosion.

ARTICLE HISTORY
Received : 29th May 2023
Revised : 28th June 2023
Accepted : 25th Sept. 2023
Published : 21st Dec. 2023

KEYWORDS
Concrete cover,
Fibrous high strength concrete,
Steel fiber,
Spiral cracks,

1.0 INTRODUCTION

Fibrous high strength concrete is a concrete with a compressive strength greater than 41 MPa that contains steel fibres to improve ductility [1]. Due to the incorporation of fibre, the brittleness index of fibrous high strength concrete is reduced [2]. In non-fibrous concrete pillars, concrete provides the pre-cracking torsional resistance. In contrast, post-cracking torsional resistance is provided solely by reinforcement [3]. In contrast, fibrous high strength concrete beams behaved similarly to fibrous normal strength concrete beams under pure torsional loading, except that fibrous high strength concrete had a higher principal tensile strength. In addition, reinforcement and fibre contribute to post-cracking torsional resistance [4]. Even though the elements that contribute to resisting torsion in non-fibrous and fibrous concrete differ only in the incorporation of fibre, the thickness of the concrete cover improves torsional resistance at crack and peak loads [5]. In contrast, the spall-off concrete cover under torsional loading is either negligible or nonexistent in fibrous concrete compared to non-fibrous concrete [1, 6]. The contribution of steel reinforcement to resist torsion was found to be diminished for under-reinforced fibrous normal strength concrete columns with a thick concrete cover. In fact, the contribution of fibre prior to and following fracture has increased [5]. In contrast, for non-fibrous concrete beams, a large concrete cover tends to spall off, whereas the torsional resistance of concrete beams with a thin concrete cover appears to be over-strengthened [9]. Consequently, it is essential to investigate the effect of concrete cover on the torsional resistance prior to and after fracture in un-reinforced high strength concrete beams. This paper focuses on the contribution of concrete cover to torsion resistance at crack and peak pressures. In fibrous high-strength concrete, the thickness of the concrete cover had a direct effect on the concrete strain at the fibre and reinforcement extremes. Therefore, the space truss model is unsuitable for evaluating torsional resistance as a result of tension stiffening in reinforcement and the conversion of the stress condition in concrete's extreme fibre from compression to tension.

Beam B-1-H is an under-reinforced fibrous high-strength concrete beam that serves as the control beam. Covers of varying thicknesses are applied to the last three beams, which have the designations C-1-H, C-2-H, and C-3-H correspondingly. They were made in a manner that was completely compliant with the standard ACI-318 [1]. The thickness of the concrete cover was varied throughout the experiment, with values ranging from 17 millimeters to 53 millimeters. During this time, the span-to-depth ratio of the section was kept at 5.72, and the aspect ratio was kept at 1.22. The beam was subjected to a pure torsional moment as a result of two-point loads that acted at the ends of the loading arms. The load was transformed into a straightforward torsional moment on the primary beam. The following sections explain the components and their relative amounts. Following that, an explanation of specimen preparation before and following testing was provided.

1.1 Materials and mix proportion between ingredients

The materials were chosen based on the ACI recommendation for fibrous concrete [10, 11]. Type I Portland cement (Tasek brand) was used. Quartz sand and crushed stone were used. Tap water, high-range water reducer Sika VC 2199, retard-admixture Plastiment R with two sizes of micro steel fiber were used. The mixed proportion of the ingredients used for the production of fibrous high-strength concrete with grade 55 MPa is shown in Table 1.

***CORRESPONDING AUTHOR | F. R. Karim|** ✉ ferhad.karim@univsul.edu.iq
© 2023 The Author(s). Published by Universiti Malaysia Pahang Publishing. This is an open access article under the CC BY-NC 4.0 license

Table 1. Mix proportion of UHPFRC

Materials	Quantity, kg/m3
Cement (Type I)	511.1
Silica sand	680.55
Crushed stone	833.33
Water	207
Water reducing super-plasticizer VC2199	10.22
Retard-admixture (Plastiment-R)	2.55
Micro steel fibre A (21mmX 0.35mmΦ)	21.59
Micro steel fibre B (12mm X 0.20mmΦ)	64.76
Slump-flow, mm	190

Φ: diameter of fibre

Silica sand was used for casting steel fiber high-strength under reinforced concrete beams. Table 2 and Table 3 show the grading and some physical properties of the silica sand. This sand complied with the limits [12-15].

Table 2. Grading of silica sand

Sieve size, mm	% Pass	ASTM limits	
		lower	upper
9.52	100.00	100	100
5.00	99.25	95	100
2.36	98.98	80	100
1.18	91.52	50	85
0.60	63.74	25	60
0.30	26.90	10	30
0.15	8.63	2	10
Fineness modulus			2.109
Average sieve size, (mm)			0.300-0.600

Table 3. Physical properties of silica sand

No.	Physical properties	Result
1	Total evaporation moisture content	0.446%
2	Absorption	1.169%
3	Relative specific gravity	2.592
4	Bulk dry density, (kg/m^3)	1536
5	% clay	3.12

1.2 Proportioning of Beam specimens

The dimensions of the beams were determined using the ACI 318 building code during the design process. In Table 4, the dimensions are tabulated. The width and depth of the stirrup in the main beam were maintained at 166 mm and 216 mm, respectively. As shown in Figures 1 and 2, the distance between stirrups remained constant at 95 mm. As longitudinal reinforcement, four 12 mm diameter bars and rectangular stirrups with 135° standard hooks were used.

Table 4. Details of the beams designed based on ACI 318 [5]

Beam designation	Concrete cover, mm	Width, mm	Height, mm **	Span length, mm*
B-1-H	28	222	272	1584
C-1-H	17	206	256	1459
C-2-H	27	234	284	1599
C-3-H	53	278	328	1886

*: span to depth ratio is around 5.72 **: aspect ratio of the section is in the range of 1.22

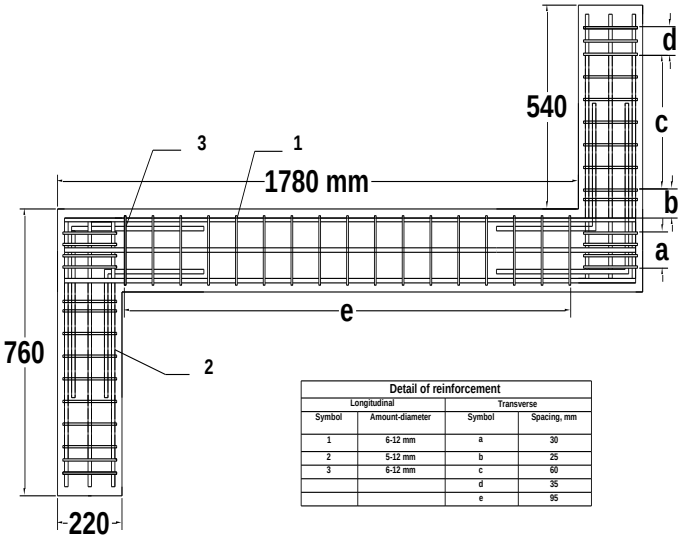

Detail of reinforcement			
Longitudinal		Transverse	
Symbol	Amount-diameter	Symbol	Spacing, mm
1	6-12 mm	a	30
2	5-12 mm	b	25
3	6-12 mm	c	60
		d	35
		e	95

Figure 1. Detail of reinforcements in the beams

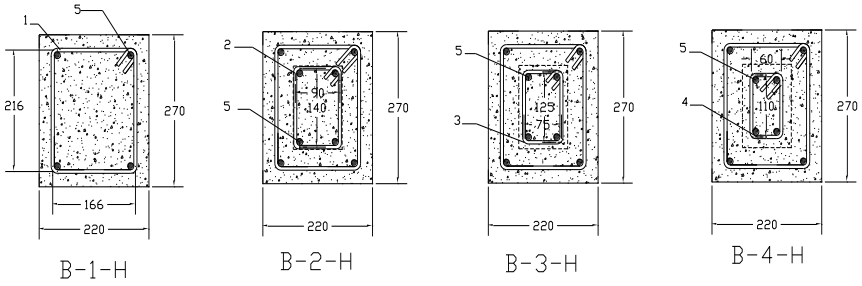

Detail of reinforcement			
No.	diameter-mm	Spacing-mm c/c	size of stirrup-mm
1	6.17	95	166 X 216
2	6.17	42.5	90 X 140
3	6.17	42.5	75 X 125
4	6.17	42.5	60 X 110
5	4-12 mm longitudinal reinforcement		

Figure 2. Details of reinforcement in the idealized core zone

2.0 SPECIMEN PREPARATION

Two pan mixers with a capacity of 0.05 m^3 were utilised for casting fibrous high-strength concrete. Figure 3 depicts the sequence for adding materials to the mixer with elapsed time to produce uniform fibrous high strength concrete. In a mould containing 3 cylinders for compression test, 3 cylinders for split tension test, 3 prisms for flexural test, and 6 cubes for bond test, fibrous high-strength concrete beams were cast with 45 seconds of vibration [16-19].

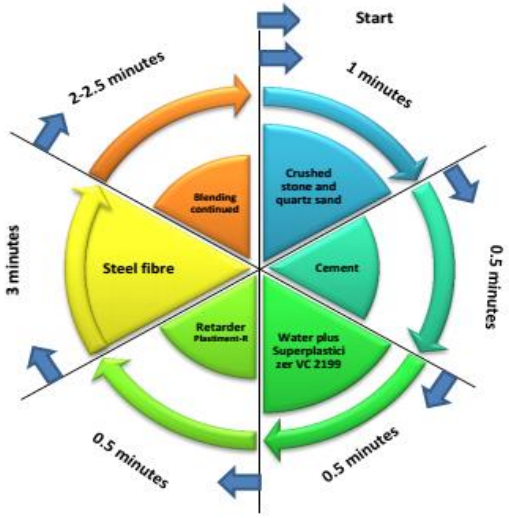

Figure 3. Schematic for mixing materials

3.0 TESTING OF BEAMS

In the Heavy Structure laboratory at USM's School of Civil Engineering, fibrous high-strength concrete beams were loaded using a universal testing machine with a 50-ton capacity. The load spreader beam received the load directly. Due to the saddle support's free movement in one direction, the load acting at the end of the loading arm that produced a bending moment in the joint between the loading arms and the main beam was changed into a torsional moment for the main beam. Thus, only a torsional moment was used to test the main beams. Figures 4 and 5 depict how the loading arrangement is set up. Two LVDTs were used to measure the twisting angle while the main beam was being loaded, 15 cm away from the joint, on the steel frame that was supported by the main beam, as shown in Figure 6. Electrical strain gauges and LVDTs were used to measure the axial strain in the transverse and longitudinal reinforcements as well as the strain in the concrete's extreme fibre. The hydraulic jack was used to manually apply the load until the beam broke under pure torsion. A load cell was used to record the load.

The load was distributed to the fibrous concrete beams using a load spreader beam of size W1049 that was seated on two load cells and roller seats, as shown in Figure 4. This was done in order to apply line load to the arms. Following that, the shear force and bending moment resulting from the line load were applied to the arms of the main beam. After that, the torsional moments in the main beam were changed to reflect the inverted bending moments in the arms.

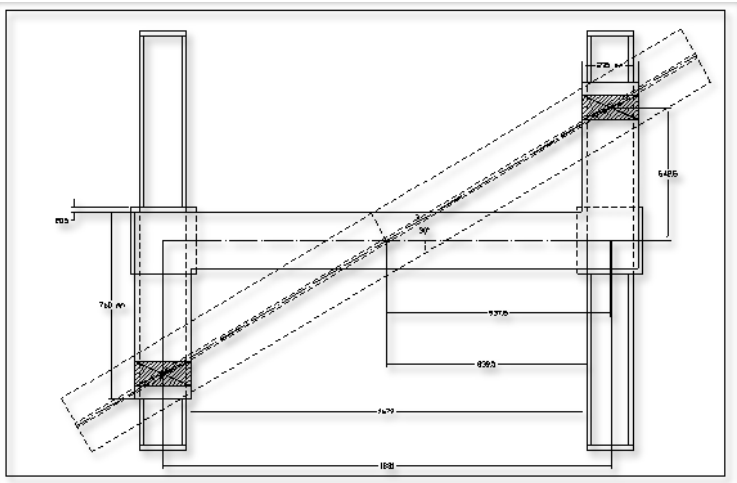

Figure 4. Schematic Test set-up

The beams were mounted on two saddle supports, with one of the supports being movable in a direction that was perpendicular to the longitudinal axis of the beam and the other support being fixed in place. In addition, the distance between each pair of supports was determined by the span length of the fibrous concrete beams, which ranged anywhere from 1645 to 2175 millimetres. The load was applied by the hydraulic jack with a capacity of 50 tonnes, which had reference code 4482. It had a loading rate of 2 kN/min, and it caused the arms to produce bending moment and shear, as shown in Figure 5. In addition, the vertical force that was produced by the loading arms was a shear force, and it did not have any effect on the main beam. On the other hand, the ability of the saddle supports to rotate inverted the bending moment that was present in the loading arms into a torsional moment that was present in the main beam.

Figure 5. Experimental setup of the beam

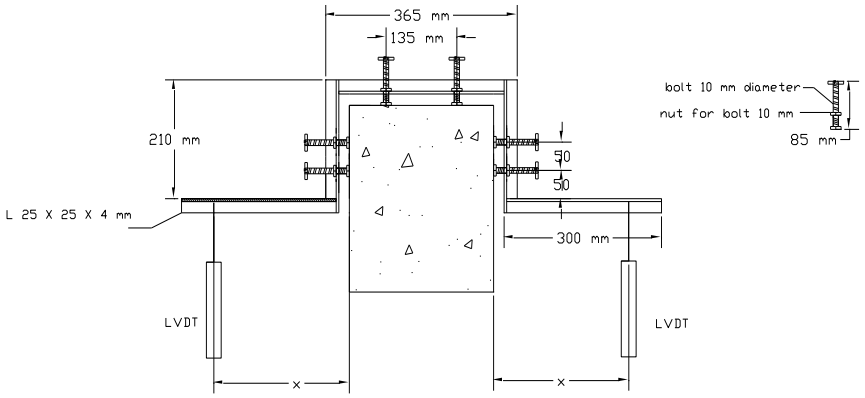

Figure 6. Schematic measuring of twisting angle

4.0 EXPERIMENTAL RESULTS

Under purely torsional loading, the fibrous high strength concrete beams were tested. During testing, a load cell and an LVDT were used to measure, respectively, the torsional resistance and the twisting angles. Furthermore, as shown in Tables 5 and 6, the angle of the crack at failure was measured.

In the sections that follow, it is discussed how the thickness of the concrete cover affects the torsional resistance at crack and peak loads, the torsional resistance offered by reinforcement and fibre, twisting angle, shear strain in concrete struts, strain in transverse and longitudinal reinforcements, and specifics of spiral cracks.

Table 5. Properties and details of the beams

Beam designation	Cylinder compressive strength, MPa	Split tensile strength, MPa	Flexural strength, MPa	Bond strength, MPa	
				Transverse reinforcement	Longitudinal reinforcement
B-1-H	62.1	8.71	8.51	4.87	10.72
C-1-H	59.2	7.44	8.99	5.04	10.84
C-2-H	58.7	7.68	7.25	5.11	10.42
C-3-H	59.0	8.14	8.11	4.95	11.07

Table 6. Results of pure torsion test in UHPFRC beams

Beam	Torsional resistance at crack load, kN.m	Twisting angle at crack load, rad/m X 10-3	Torsional resistance at peak load, kN.m	Twisting angle at peak load, rad/m X 10-3
B-1-H	21.09	1.606	26.92	11.328
C-1-H	14.59	1.109	21.80	14.124
C-2-H	18.11	1.591	22.99	5.307
C-3-H	28.23	1.122	39.39	4.206

4.1 Torsional resistance before and after cracking

Torsional resistance at crack and peak loads increased by up to 93.4% and 80.6%, respectively, as the thickness of the concrete cover increased from 28 mm to 53 mm. Figures 7 and 8 show that the compressive strength of fibrous, high strength concrete had only a minor effect on crack load torsional resistance. Meanwhile, as shown in Figure 9, the torsional resistance provided by reinforcement and fibres improved up to 54.9% due to increased concrete cover thickness.

4.2 Torsional moment and twisting angle

The torsional stiffness of the fibrous concrete beam section was significantly enhanced by a 553% increase when the concrete cover thickness was increased from 17 to 53 mm, resulting in a reduction of the twisting angle by up to 70.2%. Despite the consistent application of reinforcement and span-to-depth ratio across all sections of the beam, it was noticed that the twisting angle exhibited an inverse relationship with the stiffness of the section at the ultimate load. In contrast, there was a slight change in the twisting angles at the cracking load, despite the improvement in torsional stiffness of the section by up to 91.2%. This improvement can be attributed to the plasticity factor of the beams, which remained within the range of 0.50. The concept of plasticity was introduced by Wang and Hsu (1997) [20] and formulated in the following manner:

$$FOP = 0.8 - \frac{f_{c\prime}}{200}$$

where,

FOP: Factor of plasticity of the concrete

Figure 10 illustrates the correlation between the twisting angle and torsional moment observed during the pure torsion test conducted on the beams.

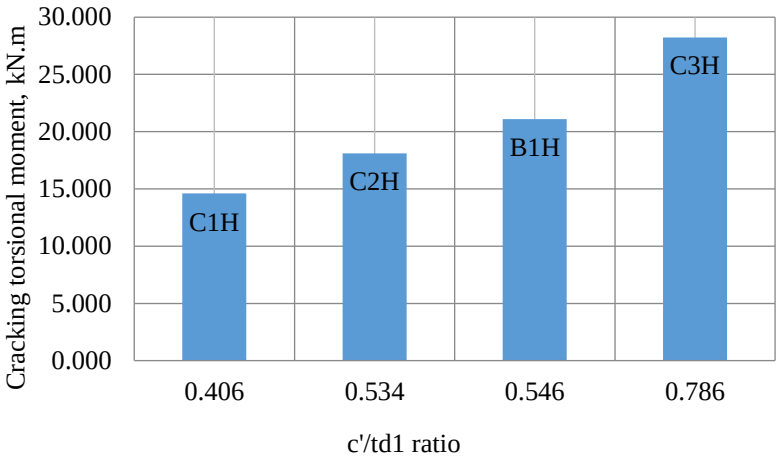

Figure 7. Effect of concrete cover on the cracking torsional resistance

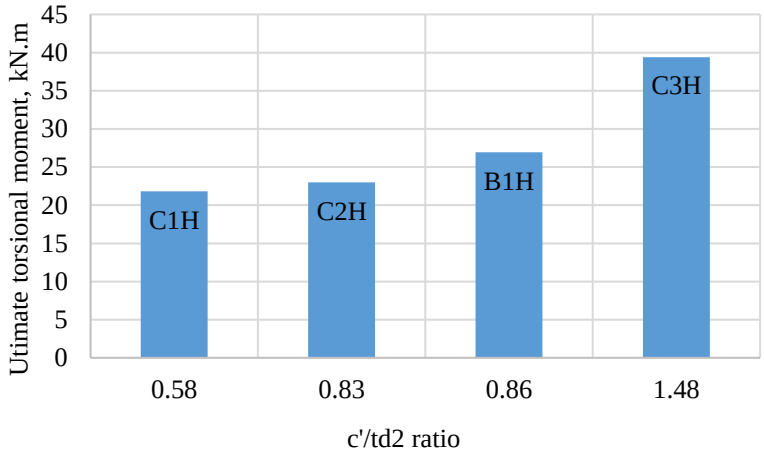

Figure 8. Effect of concrete cover on the cracking torsional resistance

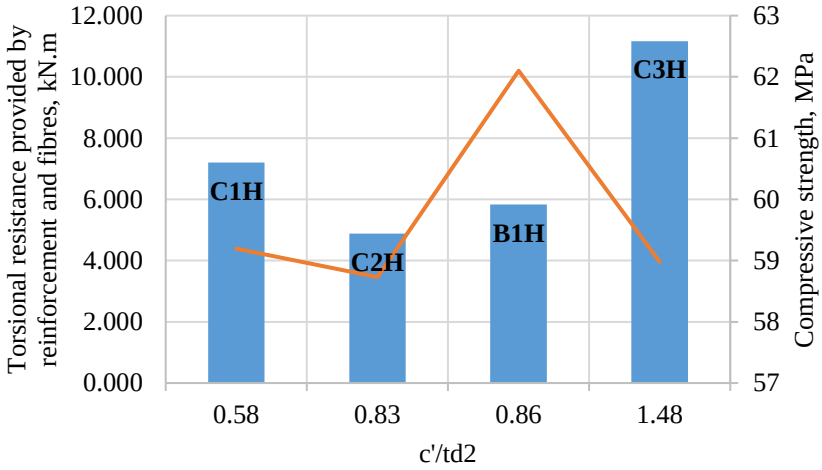

Figure 9. Effect of concrete cover on the torsional resistance provided by reinforcements and fibre

4.3 Strain in concrete and reinforcements

Concrete shear strain, transverse reinforcement strain, and longitudinal reinforcement strain all experienced reductions of up to 90%, 50%, and 35%, respectively. Figures 11–13 display the change in strain for the concrete and reinforcements. These strain reductions resulted from the tension stiffening effect. As a result, reinforcement made a smaller contribution to torsion resistance.

As can be seen in Figure 11, the concrete cover thickness had an effect on the shear strain that was measured in the concrete during the test of the beam. According to the information presented in this figure, the shear strain at the crack load was increased as a result of an increase in the cross sectional area, as was the case with the beam C-3-H.Shear strain, on the other hand, was measured at a lower value in beam C-1-H due to the beam's smaller cross sectional area. However, due to the high value of strain in the longitudinal reinforcement, the shear strain in the fibrous concrete beam at peak load had a higher value in C-1-H than in C-3-H.

As can be seen in Figures 12 and 13, the thickness of the concrete cover had an effect on the strains that were present in the transverse and longitudinal reinforcements of the fibrous high strength concrete beams. According to Figure 13, the thickening of the concrete cover prior to the cracking did not have an effect on the strain that was present in the stirrup. On the other hand, the strain was decreased even at the point of maximum load as a result of the expansion of the concrete cover, as seen in beam C-3-H. Even though there was only a thin layer of concrete covering the stirrup, as was the case with beams C-1-H and C-2-H, the strain in the stirrup increased and reached its yield strength.

In contrast, the strain in the transverse and longitudinal reinforcements at ultimate load decreased by up to 50.6% and 34.5%, respectively, as a result of an increase in the concrete cover thickness from 17 to 53 millimetres. Therefore, the contribution of the reinforcements to the effort required to resist the torsional moment was decreased to an amount that was less than or equal to half of the torsional resistance provided by reinforcements. Concrete's extreme fibres experienced a shift from compression to tension in the stress. Therefore, not all of the section can be represented using the space truss analogy. The inner part of the section was able to conduct a space truss model on that part of the section that was under compression, and the outermost part of the section operated as a hollow section under tension [5].

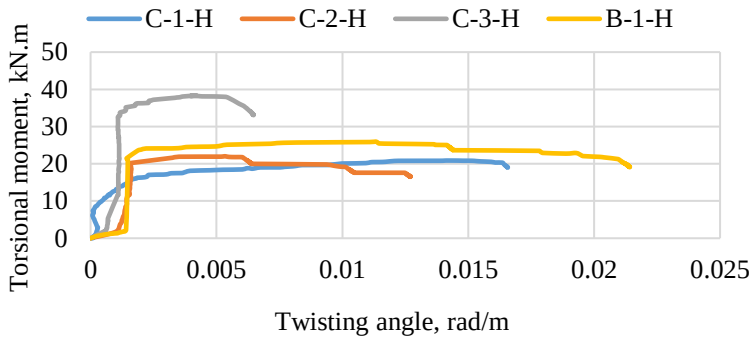

Figure 10. Torsional resistance versus twisting angle

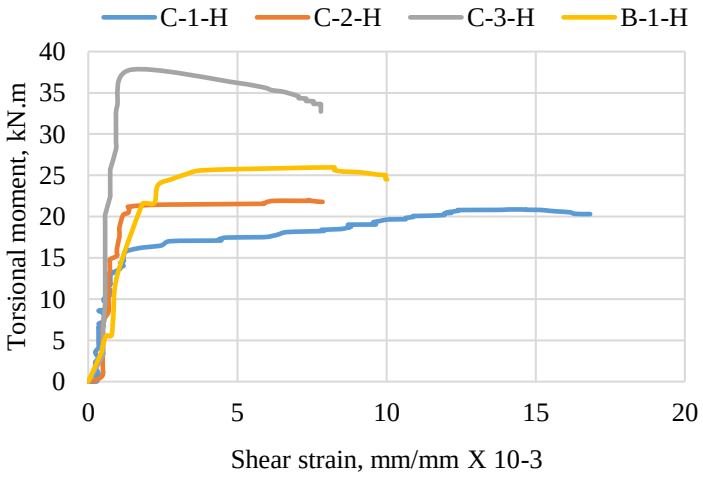

Figure 11. Torsional resistance versus shear strain in concrete

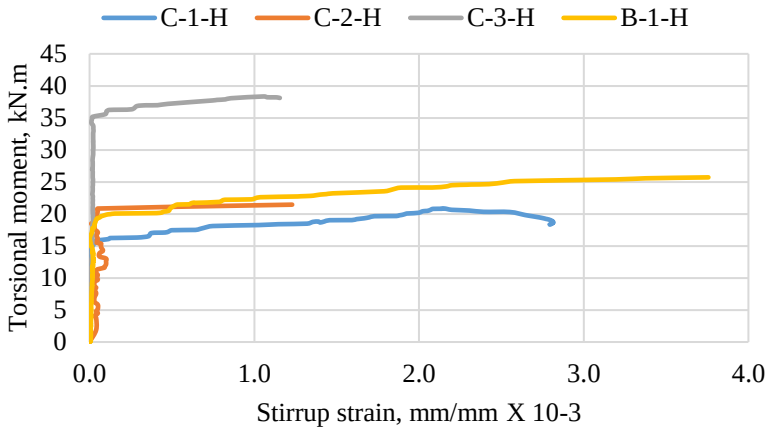

Figure 12. Torsional resistance versus strain in longitudinal reinforcement

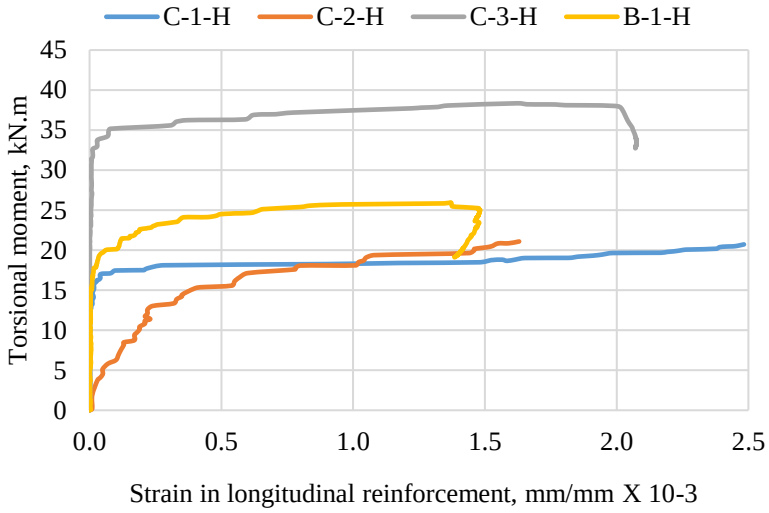

Figure 13. Torsional resistance versus strain in transverse reinforcement

4.4 Detail and crack patterns

As can be seen in Table 7, the thickness of the concrete cover had an impact on the quantity of spiral cracks, the typical distance between cracks, and the inclusion angle between cracks. It was found that as the concrete cover widened, the distance between spiral cracks grew. Therefore, there were fewer cracks. The thickness of the concrete cover had an impact on the crack patterns, as shown in Figures 14–17. The figures show that the likelihood of continuing spiral cracks increased as the concrete cover thickened.

Table 7. Detail of spiral cracks

Beam	No. of spiral cracks	Θ, degrees	Average spacing between spiral cracks, mm
B-1-H	7	46	178
C-1-H	6	49	229
C-2-H	3	47	363
C-3-H	4	43	488

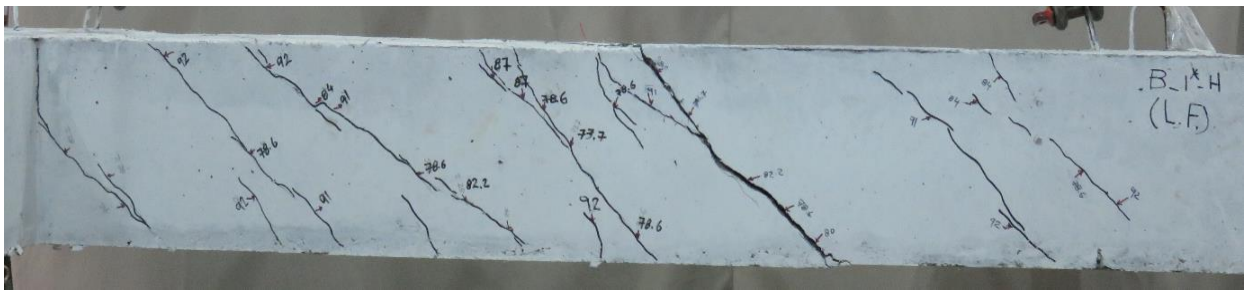

Figure 14. Crack patterns of beam B-1-H

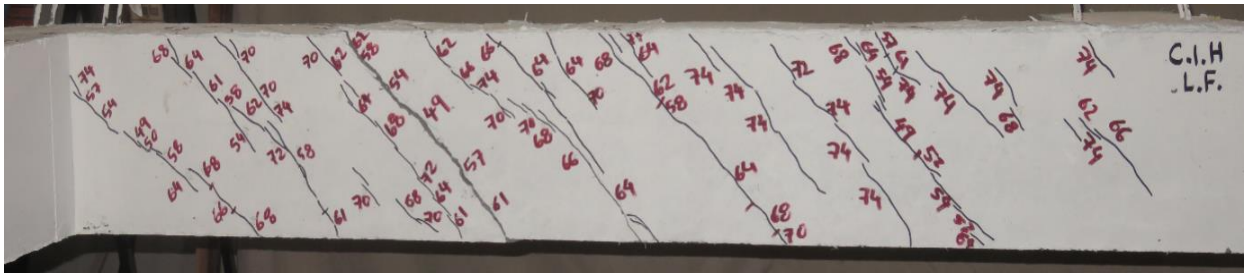

Figure 15. Crack patterns of beam C-1-H

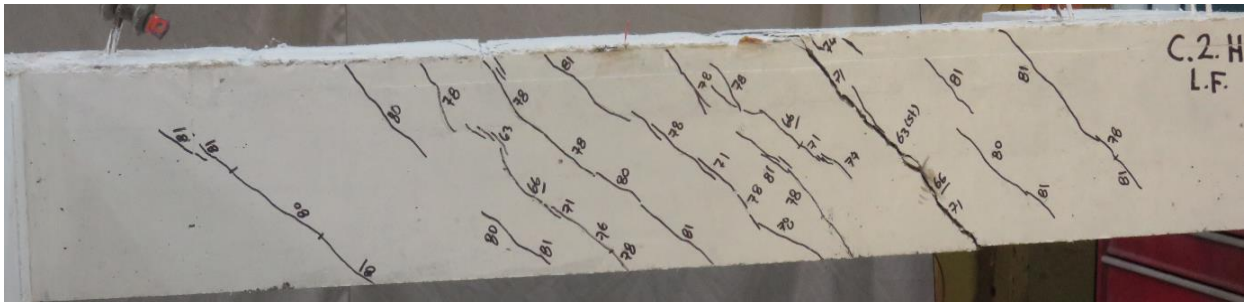

Figure 16. Crack patterns of beam C-2-H

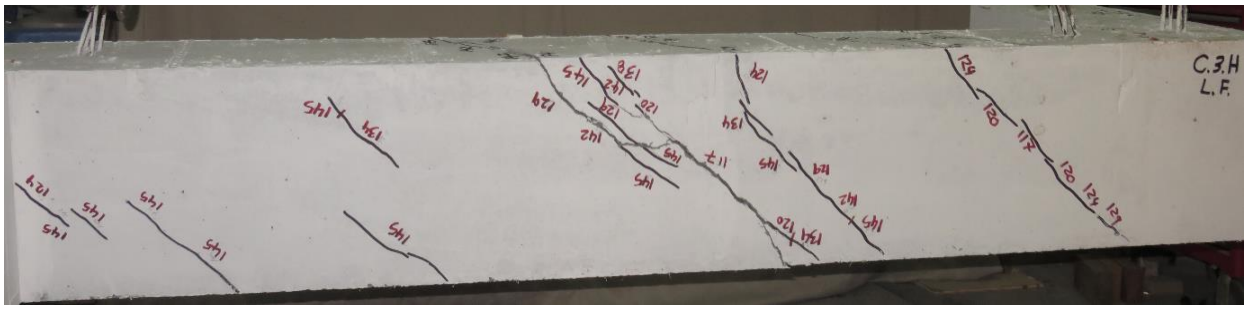

Figure 17. Crack patterns of beam C-3-H

5.0 CONCLUSION

The following conclusions can be drawn from the torsional test results on under-reinforced high-strength fibrous concrete beams:

- The torsional resistance provided by reinforcements and fiber, in addition to the torsional resistance in crack load, was improved by increasing the thickness of the concrete cover from 28 mm to 53 mm, respectively.
- Due to the boosted concrete cover thickness from 17 to 53 mm, the axial strain in the stirrup, axial strain in longitudinal reinforcement, shear strain in concrete, and twisting angle at peak load decreased by up to 50.6%, 34.5%, 90%, and 70.2%, respectively.
- The thick concrete cover widened the gap between spiral cracks. As a result, the number of spiral cracks was reduced.
- The increased thickness of the concrete cover changed the state of stress in the concrete's extreme fibre from compression to tension. As a consequence, the space truss model is not applicable to the whole beam section.

6.0 AUTHOR CONTRIBUTIONS

Ferhad Rahim Karim: Conceptualization, Methodology, Data curation, Writing- Original draft preparation, Writing-Reviewing and Editing.

Badurul Hisham Abu Bakar: Supervision.

Choong Kok Keong: Supervision.

Omar Qarani Aziz: Supervision.

7.0 FUNDING

This research was carried out as part of the first author's doctoral studies. Kurdistan Government Region-Iraq and Universiti Sains Malaysia have both provided financial support for the PhD programme.

8.0 DATA AVAILABILITY STATEMENT

The data used to support the findings of this study are included within the article.

9.0 ACKNOWLEDGEMENT

The authors would like to thank the School of Civil Engineering and all technicians at the Concrete and Heavy Structure Laboratories for providing the experimental facilities.

10.0 CONFLICTS OF INTEREST

The authors declare no conflict of interest.

11.0 REFERENCES

[1] American Concrete Institute. 318, "Torsional strength," in Building Code Requirements for Structural Concrete (ACI 318M-19) and Commentary (ACI 318RM-19), ed USA: American Concrete Institute, 2019, pp. 371-378.

[2] M. I. Rjoub and M. A. Musmar, "Toirsional strength of steel fiber reinforced concrete," *Journal of Engineering Sciences*, Assiut University, vol. 35, pp. 1-7, 2007.

[3] M. P. Collins and D. Mitchell, "Shear and torsion design of prestressed and non-prestressed concrete beams," *PCI Journal*, vol. 25, pp. 32-100, 1980.

[4] O. Fuad and E. Sekan, "Torsional behavior of steel fiber reinforced concrete beams," *Construction and Building Materials Journal*, vol. 28, pp. 269-275, 2012.

[5] F. R. Karim, B. H. Abu Bakar, C. Kok Keong, and O. Q. Aziz, "Enhancement of torsional resistance in fibrous normal strength concrete beams," *International Journal of Research in Engineering and Technology*, vol. 5, pp. 123-132, 2016.

[6] A. F. Namiq, "Effect of steel fibre on the strength and behavior of non-circular solid and hollow cross section beams under pure torsion," M.Sc., Civil Engineering Department, University of Salahaddin, Erbil, Iraq, 2012.

[7] F. R. Karim, B. H. Abu Bakar, C. Kok Keong, and O. Q. Aziz, "The enhancement of ultimate torsional resistance of under-reinforced fibrous, high strength concrete beams by the thickness of concrete cover," *Journal of Engineering and Computer Sciences*, vol. 3(1), pp. 12-22, 2020.

[8] F. R. Karim, B. H. Abu Bakar, C. Kok Keong, and O. Q. Aziz, "Review on behaviour of under-reinforced shallow fibrous concrete solid beams under pure torsion," *International Journal of current Advanced Research*, vol. 6(7), pp. 4924-4932, 2017.

[9] T. T. C. Hsu and Y. L. Mo, "Softening of concrete in torsional members-design recommendations," *ACI Journal*, vol. 82, pp. 443-452, 1985.

[10] A. C. R-93, "Guide for specifying, Proportioning, Mixing, Placing, and Finishing Steel Fiber Reinforced Concrete," American Concrete Institute, vol. 544.3R, 1998.

[11] A. C. R-98, "Guide to Quality Control and Testing of High Strength Concrete," American Concrete Institute, vol. 363.2R, 1998.

[12] ASTM-C33/C33M. Standard Specification for Concrete Aggregates. Annual book of ASTM standard, C33/C33M, 4.02, 2013.

[13] ASTM-C29/C29M. Standard Test Method for Bulk Density ("Unit Weight") and Voids in Aggregate. Annual book of ASTM standard, C29/C29M, 4.02(C29/C29M), pp. 1-5, 2009.

[14] ASTM-C70. Standard Test Method for Surface Moisture in Fine Aggregate. Annual book of ASTM standard, C70, 4.02(C70), pp. 38-40, 2006.

[15] ASTM C566. Standard Test Method for Total Evaporable Moisture Content of Aggregate by Drying. Annual book of ASTM standard, C566, 4.02(C566), pp. 315-317, 2004.

[16] ASTM-C39/C39M, "Standard Test Method for Compressive Strength of Cylinderical Specimens," Annual book of ASTM standard, vol. 4.02, pp. 23-29, 2010.

[17] ASTM-C496/C496M, "Standard Test Method for Splitting Tensile Strength of Cylinderical Concrete Specimens," Annual book of ASTM standard, vol. 4.02, pp. 299-303, 2004.

[18] ASTM-C1609/C1609M, "Standard Test Method for Flexural Performance of Fiber-Reinforced Concrete (Using Beam with Third-Point Loading," Annual book of ASTM standard, vol. 4.02, pp. 846-854, 2010.

[19] IS:2770, "Methods of Testing Bond in reinforced concrete: Pull-out test," Bureau of Indian Standards, vol. 2770, pp. 1-10, 2007.

[20] W. Wang, and Th. T.C. Hsu, “Limit Analysis of Reinforced Concrete Beams Subjected to Pure Torsion,” *Journal of Structural Engineering*, vol. 123(1), pp. 86-94, 1997.